ACS Photonics

Article

pubs.acs.org/journal/apchd5

Constructing "Designer Atoms" via Resonant Graphene-Induced Lamb Shifts

Cyuan-Han Chang,[†] Nicholas Rivera,*[,†] John D. Joannopoulos,[†] Marin Soljačić,[†] and Ido Kaminer[†,‡]

[†]Department of Physics, Massachusetts Institute of Technology, Cambridge, Massachusetts 02139, United States

[‡]Department of Electrical Engineering, Technion − Israel Institute of Technology, Haifa 32000, Israel

Supporting Information

ABSTRACT: The properties of an electron in an atom or molecule are not fixed; rather they are a function of the optical environment of the emitter. Not only is the spontaneous emission a function of the optical environment, but also the underlying wave functions and energy levels, which are modified by the potential induced by quantum fluctuations of the electromagnetic field. In free space, this modification of atomic levels and wave functions is very weak and generally hard to observe due to the prevalence of other perturbations like fine structure. Here, we explore the possibility of highly tailorable electronic structure by exploiting large Lamb shifts in tunable electromagnetic environments such as graphene, whose optical properties are dynamically controlled via doping. The Fermi energy can be chosen so that the Lamb shift is very weak, but it can also be chosen so that the shifts become more prominent than the fine structure of the atom and even potentially the Coulomb interaction with the nucleus. Potential implications of this idea include being able to electronically shift an unfavorable emitter structure into a favorable one, a new approach to probe near-field physics in fluorescence, and a way to access regimes of physics where vacuum fluctuations are not a weak perturbation but rather the dominant physics.

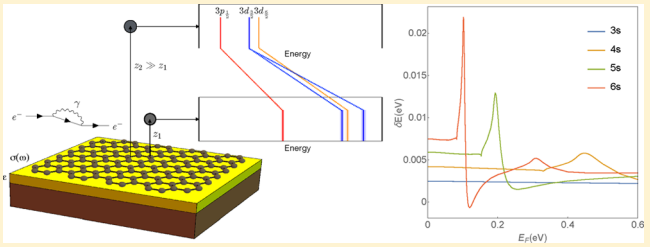

KEYWORDS: *Lamb shift, graphene plasmonics, light−matter interactions, quantum electrodynamics*

It has long been known that the quantum fluctuations of the electromagnetic vacuum have an influence on the electromagnetic properties of atoms. Not only does the electromagnetic vacuum drive spontaneous emission,[1] but it also shifts electronic energy levels and modifies electronic wave functions.[2,3] The effect can be viewed as resulting from virtual emission and reabsorption of photons. While atomic spontaneous emission had been experimentally evident for centuries, the Lamb shift had to wait until the advent of high-precision RF spectroscopy in the 1940s to claim a clear experimental footing.[3] This is because the Lamb shift is a weak effect in free space, associated with frequency shifts of about 1 GHz, over an order of magnitude weaker than the much more easily detectable fine structure.

Although the quantum fluctuations associated with the Lamb shift are a very weak effect on atoms in free space, they can be made substantially larger by placing the atom in the vicinity of a dielectric or metallic surface. This effect goes by names such as van der Waals and Casimir-Polder but is equivalent to the Lamb shift associated with quantum fluctuations of electromagnetic field modes which differ from free-space on account of the nearby surface. This effect has been well characterized both theoretically and experimentally for the case of Rydberg atoms in the vicinity of nearly perfectly conducting metallic surfaces.[4−7] Beyond these, the effect has been theoretically explored for atoms near a wide variety of optical environments such as different configurations of plasmonic materials,[8−12] metamaterials,[13] and structured dielectrics such as photonic crystals,[14−20] even with some experimental observations for photonic crystals.[21]

A limitation on the technological applications of this effect however arises from the general lack of tunability of the optical properties of the medium. One can imagine that the ability to tune the optical environment could allow for a great degree of customization over the emission, absorption, and general electronic properties of an emitter, allowing one to "tune matter" with a great degree of control. In fact, much interest has gravitated recently toward nanophotonics/nanoplasmonics in graphene, whose optical conductivity can be tailored by changing the doping level in graphene.[22−25] A number of proposals for taking advantage of this tunable plasmonic material include, but are not limited to tunable metamaterials,[26] tunable interactions with emitters,[25,27] electrically controlled perfect absorbers,[28] tuning Casimir forces for mechanical sensing,[29] tunable light sources via the plasmonic Cerenkov effect,[30] and electrical control over atomic selection rules by taking advantage of access to conventionally forbidden transitions.[31]

Special Issue: 2D Materials for Nanophotonics

Received: July 6, 2017
Published: September 12, 2017

DOI: 10.1021/acsphotonics.7b00731
ACS Photonics 2017, 4, 3098−3105

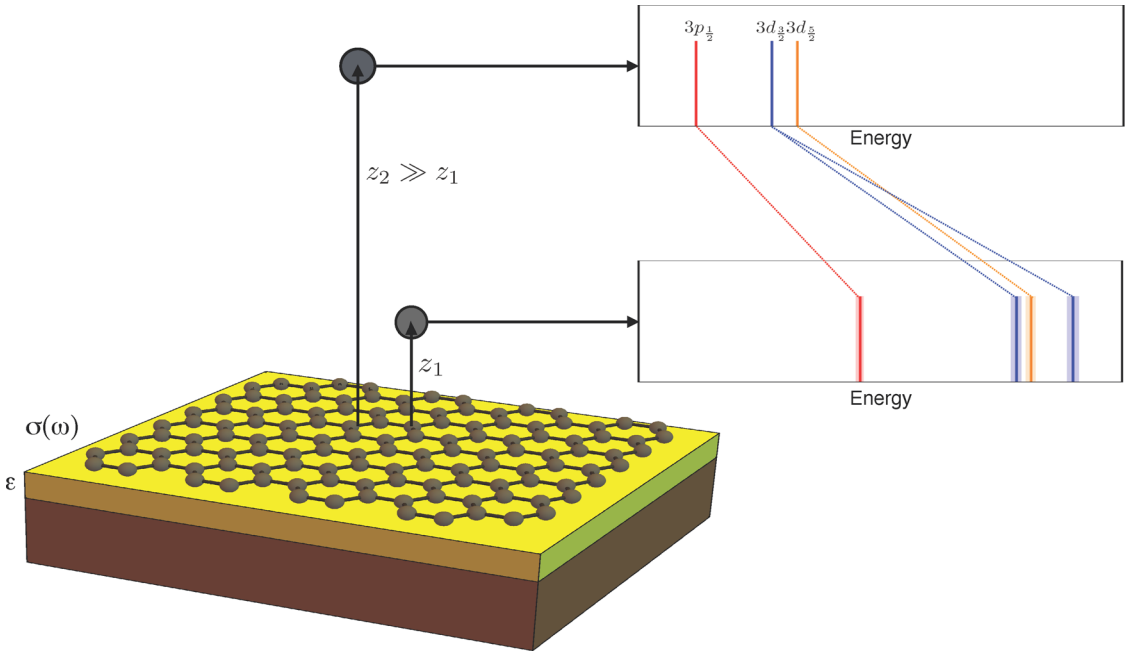

Figure 1. Schematic showing how the atomic energy levels change as the atom approaches the graphene. The levels not only shift, but also broaden due to the possibility of very fast spontaneous decay into either graphene plasmons or loss channels in graphene such as particle-hole excitations.

In this work, we explore the degree of control that can be obtained over electronic structure using the Lamb shift in graphene, for use of designing tunable emitters and absorbers, and for use in studying fundamental light-matter interactions potentially beyond the weak-coupling regime. We find a number of surprising results. For example, the dependence of the Lamb shift on the doping in graphene can be very sharp around certain "resonance" energies related to the energies of electronic transitions. At these resonance points, an emitter a few nanometers away from graphene can have a Lamb shift not only much larger than fine-structure corrections but potentially comparable to the spacing between the principal levels from the Coulomb interaction with the nucleus in the absence of graphene, signaling the onset of nonperturbative QED effects. Additionally, with the degree of freedom offered by the tunability of the Fermi energy, we can also tune the Lamb shifts to be small and relatively insignificant. These two results suggest the potential for a wide degree of control of atomic energy levels (and wave functions), suggesting the possibility of using quantum vacuum fluctuations for creating "designer" atoms.

A schematic of the proposed concept is shown in Figure 1, where we show an electronic system such as an atom, molecule, or artificial atom in the vicinity of graphene. When the atom is at a large distance z_2 away from the surface of graphene, it will have an energy spectrum which will mostly look like the spectrum in free space. As we bring the atom closer and closer to a distance z_1, its energy levels can shift substantially as a result of the Lamb shift, in addition to broadening substantially as a result of the Purcell effect associated with the large local density of states near the graphene sheet. In order to translate the proposed concept into concrete results, we calculate the Lamb shifts for both Hydrogenic atoms and two-level atoms in the vicinity of graphene. This calculation can readily be extended to other electronic systems if one knows the dipole matrix elements between the different energy states of the atom. We now briefly overview the details of the calculations, which are discussed in more detail in the Supporting Information (SI).

The energy levels and wave functions of the atom are shifted due to a perturbation Hamiltonian: $\frac{e}{2m}(\mathbf{p}\cdot\mathbf{A} + \mathbf{A}\cdot\mathbf{p}) + \frac{e^2}{2m}\mathbf{A}^2$. This perturbation Hamiltonian includes the effect of the electromagnetic modes of the optical surroundings on the atom. We have assumed that the effect of fine-structure is already included in the unperturbed Hamiltonian, which is fair assuming that these relativistic effects are unmodified by plasmons. In long-wavelength (dipole) approximation, the Hamiltonian is equivalent to $-\mathbf{d}\cdot\mathbf{E} + \epsilon_{\mathrm{dip}}$ up to a unitary transofrmation,[32] where the first term is the usual dipole coupling and the second term is the dipole self-energy term. The Lamb shift calculated using the two expressions of the Hamiltonian are the same once the dipole self-energy is included and all states are taken into account (see SI for proof). Keeping these different contributions in mind and calculating the energy shift of level a, denoted δE_a to second-order in perturbation theory yields (in repeated index notation):

$$\delta E_a = \frac{4\alpha\hbar}{c}\mathcal{P}\int \mathrm{d}\omega\omega^2 \mathrm{Im}\, G_{ij}(\mathbf{r}_0, \mathbf{r}_0, \omega)\left(\frac{(r_i r_j)^{aa}}{\omega} + \sum_b \frac{r_i^{ab} r_j^{ba}}{\omega_{ab} - \omega}\right) \quad (1)$$

where $\alpha \approx 1/137$ is the fine-structure constant, $G_{ij}(\mathbf{r}_0, \mathbf{r}_0, \omega)$ is the dyadic Green function of the optical environment at the position of the atom $\mathbf{r}_0$, $r_i^{ab} = \langle a|r_i|b\rangle$ is a position matrix element between states a and b, $(r_i r_j)^{aa} = \langle a|r_i r_j|a\rangle$ is the expectation value of $r_i r_j$ of state a, ω_{ab} is the transition frequency between states a and b, and $\mathcal{P}$ denotes the principal part. The Green function is calculated using the known expression in terms of an integral over in-plane wavevectors, taking the conductivity of the graphene as its input.[33] We note that the effect of the modes being different from free space can be accounted for separately from the effect of free space modes

DOI: 10.1021/acsphotonics.7b00731
ACS Photonics 2017, 4, 3098−3105

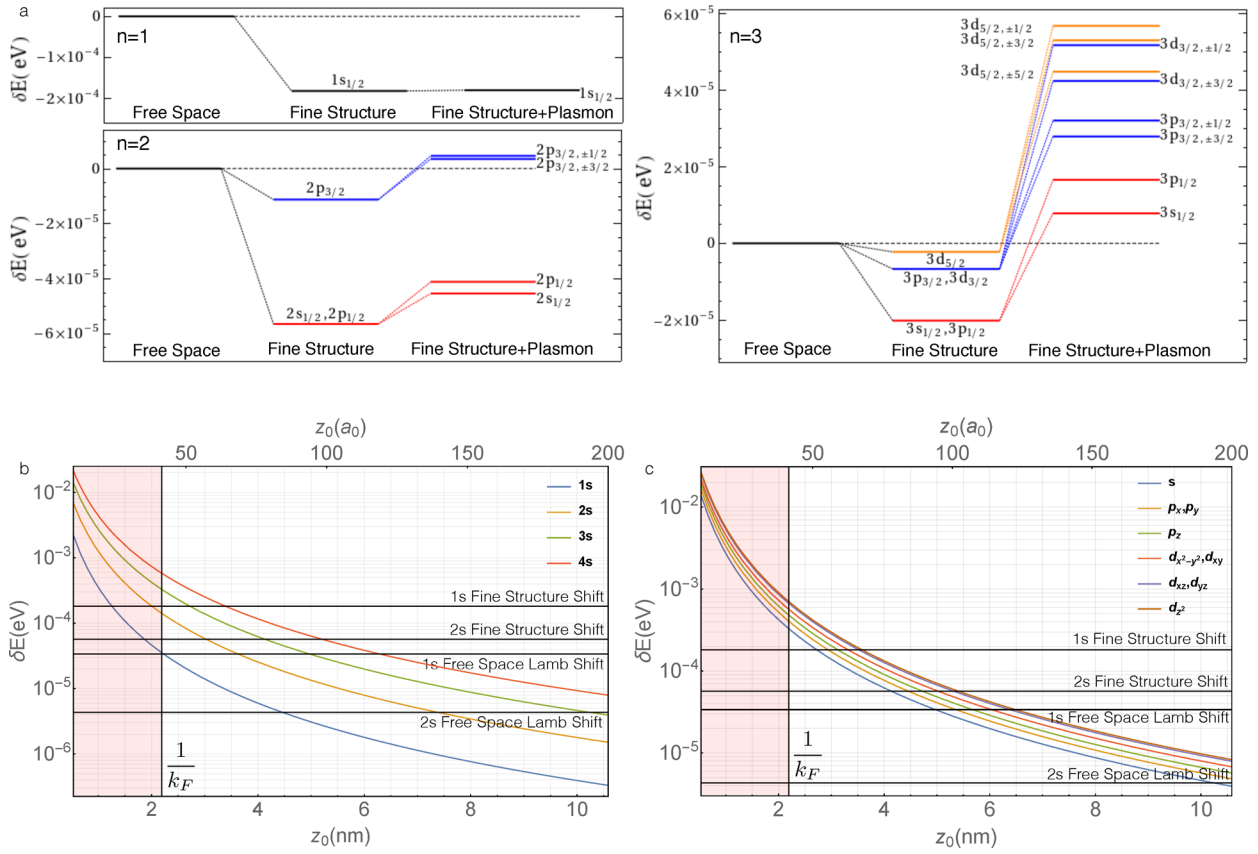

Figure 2. Magnitude of the Lamb shift of hydrogen levels near graphene: (a) Level diagrams of $n = 1$, $n = 2$, and $n = 3$ atomic states of a hydrogen atom located 5 nm away from a graphene with doping level 0.3 eV. (b) Energy shifts of 1s, 2s, 3s, and 4s states. The red area indicates when the distance is smaller than k_F^{-1}, where we expect nonlocality to kick in. (c) Energy shifts of $n = 3$ states of different angular quantum numbers and different orbital orientations. The relaxation time of graphene is taken to be 100 fs, independent of Fermi energy.

by using the scattered Green tensor in the expression above, which is the Green tensor minus its value in vacuum. We use the scattered Green tensor in this work. The entire scattered Green function contains contributions from modes with s-polarization and with p-polarization, each polarization can also be decomposed into far-field modes (real z-directed wave vector) and the evanescent modes (imaginary z-directed wave vector).[33] Even though the total energy shift has contribution from all the far-field and evanescent s- and p-polarized modes, the energy shift from the two types of far-field modes is about 10^{-6} eV, which is on the same order of magnitude as the free space Lamb shift, and also becomes much smaller than the shift from the evanescent modes as the distance decreases. We find that at short distances ($\lesssim$10 nm), the shift from the far-field modes is much smaller than the shift from the evanescent modes and can thus be ignored. Furthermore, the shift from the s-polarized evanescent mode is smaller than the shift from the p-polarized evanescent mode by a factor of η^2, where $\eta = \frac{qc}{\omega} \sim 100$ is a very high confinement factor achievable in graphene plasmons, q is the plasmon wave vector, and ω is the plasmon frequency.[25] These p-polarized evanescent modes are associated with graphene plasmons. As a result of these considerations, in what follows, we only consider the contribution from p-polarized evanescent modes in the Green function in our subsequent Lamb shift calculations.

For most parameters that we consider in this work, it is sufficient to consider the surface conductivity of graphene as being well-described by a local random phase approximation (RPA; assumed at zero temperature). In the local RPA, the complex conductivity $\sigma(\omega) = \sigma_R(\omega) + i\sigma_I(\omega)$ takes the form:[34]

$$\sigma_R(\omega) = \frac{e^2 E_F}{\pi\hbar^2}\frac{\frac{1}{\tau}}{\omega^2 + \frac{1}{\tau^2}} + \frac{e^2}{4\hbar}\theta(\hbar\omega - 2E_F) \tag{2a}$$

$$\sigma_I(\omega) = \frac{e^2 E_F}{\pi\hbar^2}\frac{\omega}{\omega^2 + \frac{1}{\tau^2}} - \frac{e^2}{4\pi\hbar}\ln\left|\frac{2E_F + \hbar\omega}{2E_F - \hbar\omega}\right| \tag{2b}$$

where τ is the collision relaxation time (taken to be 100 fs in this work), σ_R is the real part of conductivity, and σ_I is the imaginary part. In the absence of the second terms of both the real and imaginary parts, one is left with the Drude model which captures the effect of far field modes, graphene plasmons, and intraband absorption channels, but does not see the contribution of particle-hole excitations to the Lamb shift. Later in the text, we elucidate the contributions of each of plasmons, local absorption channels, and particle-hole excitations to the Lamb shift. For our analysis, we neglect the nonlocal corrections to the conductivity, which should be accurate for the distances $z_0 \geq \frac{1}{k_F}$. Thus, as a result of our adopting the local RPA, we should only consider the contribution of modes with wavevectors $q < k_F$ where k_F is the Fermi wavevector, approximately equal to $300\frac{E_F}{\hbar c}$. Above this wavevector, the response of graphene decreases. For distances $z_0 \gg \frac{1}{k_F}$, the latter of which is about 1 nm for the values of E_F of interest,

DOI: 10.1021/acsphotonics.7b00731
ACS Photonics 2017, 4, 3098−3105

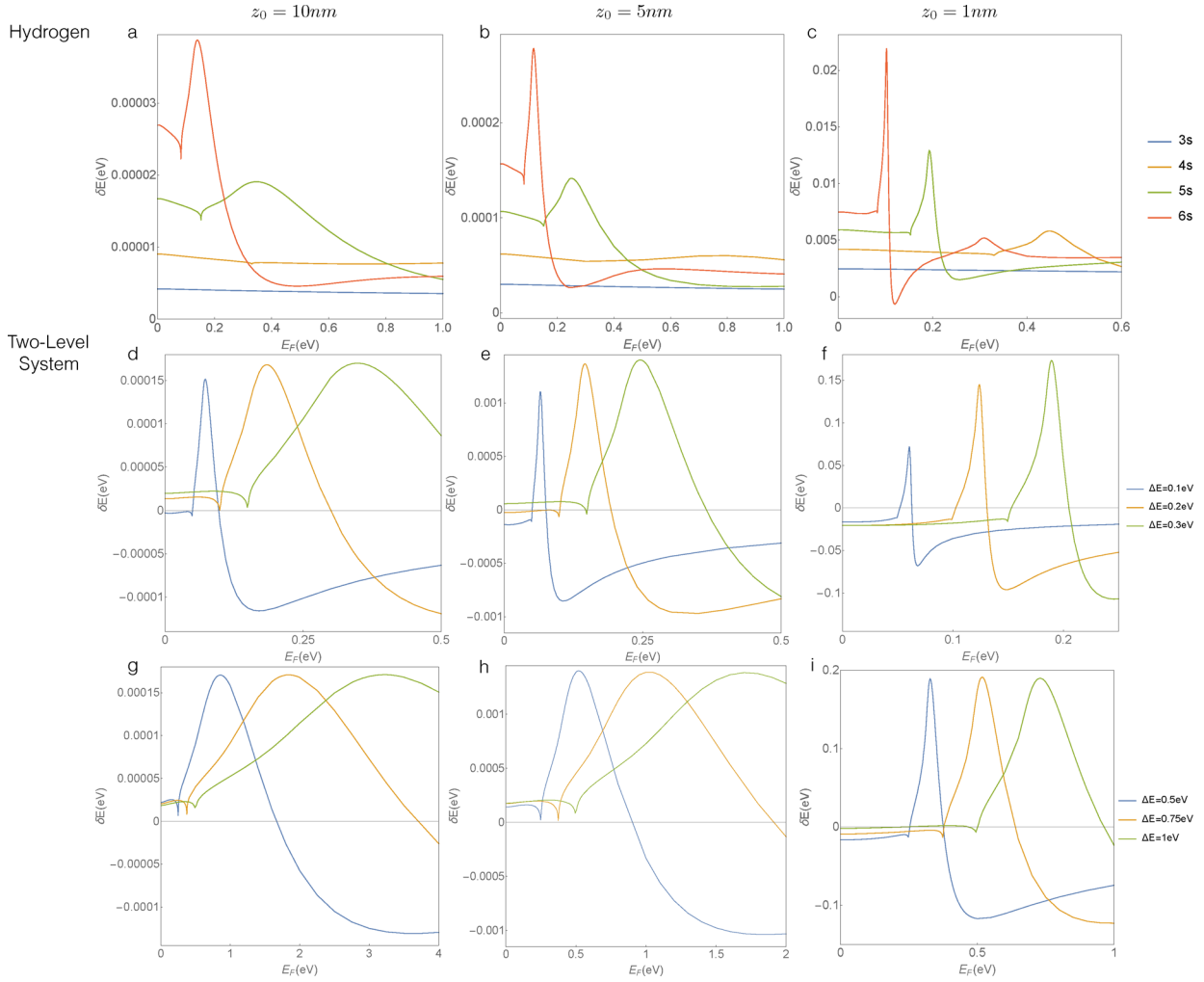

Figure 3. Resonant control over atomic energy levels with graphene: (a–c) Lamb shifts for 3s, 4s, 5s, and 6s states of the hydrogen atom as a function of the graphene Fermi energy for atom-surface separations of (a) 10 nm, (b) 5 nm, and (c) 1 nm. One can see the presence of resonances in the Fermi energy where the Lamb shift can jump sharply. The effect is strongest for the 6s states. (d–i) Lamb splitting of the energy gap of a two-level system with energy gaps of (d–f) 0.1, 0.2, and 0.3 eV, respectively, and (g–i) 0.5, 0.75, and 1 eV for atom-surface separations of 10, 5, and 1 nm, respectively. The relaxation time of graphene is taken to be 100 fs independent of Fermi energy.

these high wavevector modes are not too important due to the evanescent character of the modes contributing to the Lamb shift. Although we consider the $T = 0$ local RPA conductivity for simplicity, the frequency-dependent conductivity is similar provided that $\hbar\omega \gg k_B T$[25] and $E_F \gg k_B T$, which in our calculations works well for room temperature for most the frequencies and Fermi energies considered here. That said, the other condition needed for the scheme proposed in this work to be useful is that the emitter levels are not too broadened by the effect of temperature.

MAGNITUDE OF THE LAMB SHIFTS IN GRAPHENE

In Figure 2a, we show the effect of graphene (doped to a Fermi energy of 0.3 eV) on the energy level diagram of the Hydrogen atom held 5 nm above the surface, looking at the 4-fold degenerate $n = 2$ and the 9-fold degenerate $n = 3$ manifold. We plot the resulting level diagrams in three cases. The first case is when the atom is in free space with only the Coulomb interaction. To compare the scales of the fine structure effect and the plasmonic Lamb shift effect, we then include the fine structure shift in the second case and the total shift including both the fine structure shift and the Lamb shift is shown in the third case. Immediately it becomes clear that as the quantum number increases, the strength of the Lamb shift also increases, as a result of the increased dipole moments of higher-lying states. This of course means that the prospects of reshaping atomic energy level structure are mostly applicable to excited state manifolds, although they could be applied to ground states in artificial atoms with large dipole moments. For the $n = 3$ states, the graphene Lamb shift now exceeds the fine structure by nearly an order of magnitude, making it a potentially simple-to-observe spectroscopic effect. Additionally, the degeneracies of the states retained by the fine structure are completely split, allowing one to create a complex manifold of states starting from a highly degenerate state. In this particular example of $n = 3$, the size of the manifold is nearly on the order of 0.1 meV. This degeneracy breaking is a consequence of the asymmetry between in-plane and out of plane directions, allowing for a distinction between different orbital angular momentum projections in the direction perpendicular to the graphene normal. This degeneracy breaking would apply for for any cylindrically symmetric atom or molecule coaxial with the graphene.

DOI: 10.1021/acsphotonics.7b00731
ACS Photonics 2017, 4, 3098–3105

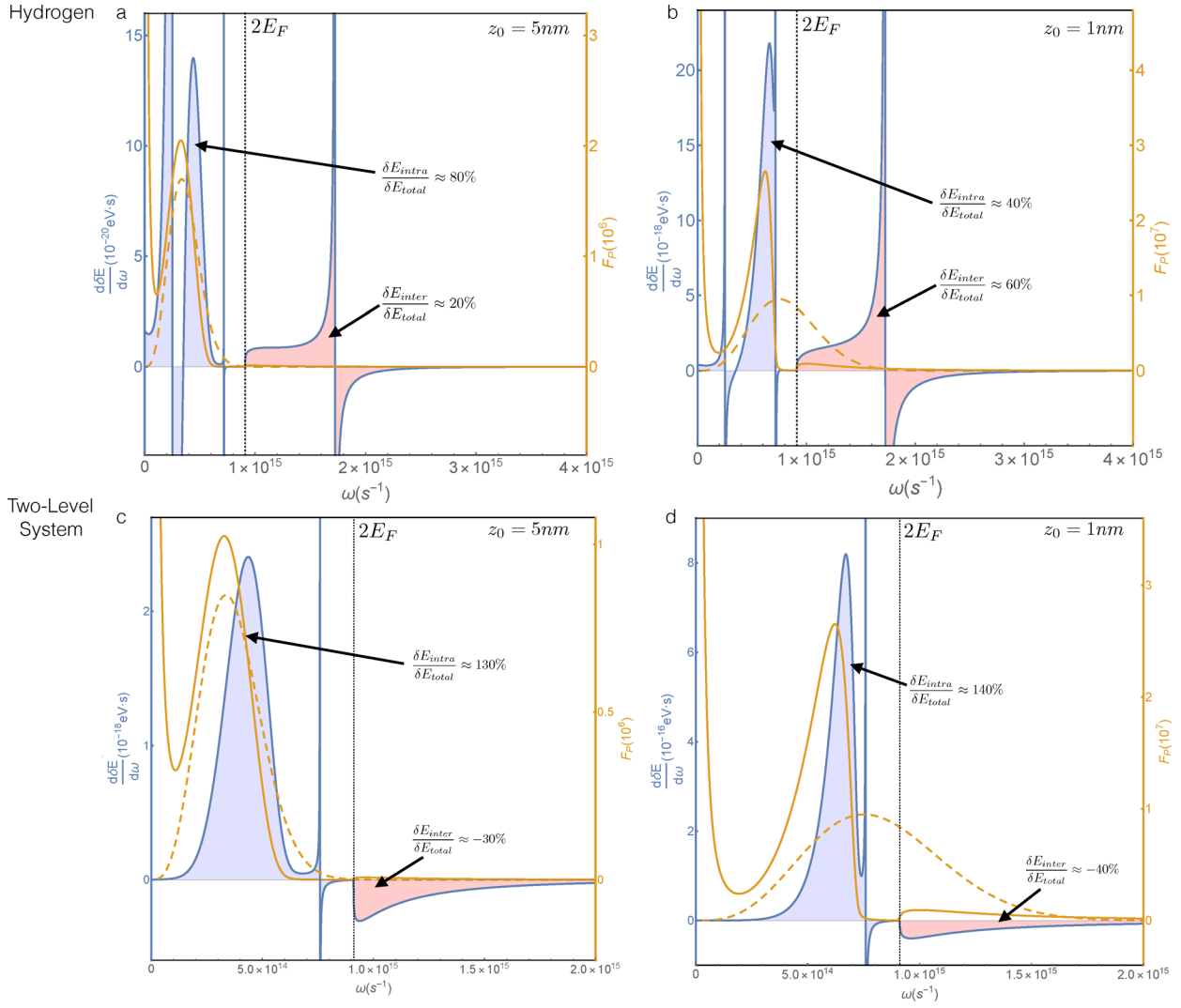

Figure 4. Plasmon and particle-hole pair contributions to the Lamb shift and origin of Fermi energy resonances. (a, b) 6s state differential Lamb shift and Purcell factor as a function of plasmon frequency, plotted at separation (a) 5 nm and (b) 1 nm, respectively. (c, d) The differential Lamb shift and Purcell factor for a two level system with energy gap 0.3 eV and dipole moment 7.4 D (1 nm charge separation) (c) 5 nm and (d) 1 nm away. The graphene doping level is E_F = 0.3 eV. The blue and red areas indicate the intraband and interband contribution, respectively. The solid lines are calculated using local RPA and the dashed lines are calculated using lossless Drude model. For the calculations including losses, a relaxation time of graphene is taken to be 100 fs independent of Fermi energy.

In Figure 2b,c, we show how the magnitude of the Lamb shift depends on the separation between the atom and graphene, and the shifts from the fine structure effects are not included. As we show in the SI, the scaling of the Lamb shift with distance goes as $1/z_0^3$, which agrees well with our results shown in the figure. Indeed, the energy shift predictions in Figure 2 increase by 2 orders of magnitude when decreasing the distance to around 1 nm. Importantly, significant Lamb shifts are apparent also much farther away from the surface (e.g., at 10 nm distance, the Lamb shift can still be the dominant mechanism of energy splitting). As a result of this sharp scaling with distance, the ability to tune matter is of course most evident at short distances (<10 nm).

CONTROLLING THE LEVEL DIAGRAMS OF ATOMS WITH THE FERMI ENERGY

Although it may be possible to use z_0 as a tuning parameter, that is often not the case because one has an emitter which is embedded and thus in a fixed position. To this end, we now consider the ability to tune the level structure of an atom that is held at a fixed position by varying the Fermi energy. In Figure 3a–c, we plot the graphene-induced Lamb shift of the 3s, 4s, 5s, and 6s levels as a function of graphene Fermi energy at three different distances, 10 nm, 5 and 1 nm, respectively. One of the most clear features that can be seen is that the shift can attain a sharp maxima, sharp minima, and even zeroes (Figure 3c) at certain values of the Fermi energy, the origin of which will be explained in the next section. As one can see from Figures 3a–c, the resonances are the sharpest for the higher-lying energy states, and they occur at smaller Fermi energies. As we will also explain in the next section, these resonance energies are related to the energy differences between adjacent energy levels.

In Figure 3d–i, we switch perspective from considering Lamb shifts in a Hydrogen atom to considering Lamb shifts in a two-level system. While there are no two-level atoms in nature, what this system approximates is a situation where one particular intermediate state captures most of the contribution to the Lamb shift due to a large dipole moment between these

DOI: 10.1021/acsphotonics.7b00731
ACS Photonics 2017, 4, 3098–3105

states. Additionally, it is a rather popular model for considering Lamb shifts and van der Waals forces in other systems, and it could potentially better approximate systems that do not have such a large degree of degeneracy as a Hydrogen atom or an alkali atom. For the calculation of the Lamb shift in a two-level system, the main difference from the Hydrogen case is the number of intermediate states in eq 1 and lack of the big energy shift contribution from the degenerate states. It also requires the specification of the dipole moment between the two states, which is taken to be about 7.4 D, corresponding to a charge separation of 1 nm. In Figure 3d–i, we consider the splitting of the energy gap of this two-level atom between the excited and ground states due to graphene as a function of Fermi energy for atom-surface separations of (d, g) 10 nm, (e, h) 5 nm, and (f, i) 1 nm. In Figure 3d–f, we consider energy gaps of 0.1, 0.2, and 0.3 eV, while in Figure 3g–i, we consider energy gaps of 0.5, 0.75, and 1 eV. What can easily be seen in all six of these panels is that the Fermi energy resonances are present, that the resonance position increases with the energy gap, and that the contrast in the Lamb shift as a function of Fermi energy is sharper than in the Hydrogenic case. In fact, we see in all six panels that tuning the Fermi energy can allow for the splitting to change sign, and consequently, can be made to vanish altogether, allowing one to effectively "turn off" the effect of the graphene on these two energy levels. Looking at the magnitude of the peaks in the Lamb shift as a function of energy, we can see that at 5 nm, the energy gap can be tuned on the scale meV, corresponding to as much as a 1% degree of tunability in the case where the energy gap is 100 meV.

Finally, we comment on the magnitude and tunability of the graphene-induced Lamb shift on an atom 1 nm away from the surface, considered in Figure 3c,f,i. When the Fermi energy is about 0.1 eV, the 6s state Lamb shift has a maximum value of about 0.02 eV. This shift is in fact about 15% of the energy difference between the 5s and 6s levels. For the two-level systems in Figure 3f, the magnitude of the shift can be over 50% percent of the energy gap. Additionally, the Fermi energy can also be adjusted so that the Lamb shift is turned off (the nodes of the curves in Figure 3), meaning that perhaps it could be possible to have a degree of control over the shift of the energy levels that spans between 0 and an amount comparable to the unperturbed energies themselves. We conclude this section by noting the results at 1 nm should be interpreted as qualitative for a number of reasons. For one, at these extremely short distances, nonlocal effects should be rigorously taken into account. Moreover, as we show in the Supporting Information, at separations of 1 nm, the wavevectors contributing to the Lamb shift become so large that multipolar corrections to the Lamb shift become relevant and in some cases even larger than the corrections from the dipole terms.[31] Finally, and potentially most interestingly, these level shifts are so large that the coupling between the atom and electromagnetic field is approaching a nonperturbative regime. A potential means for studying these effects in the nonperturbative regime could be a method proposed in ref 4, which was used to study van der Waals shifts of Rydberg atoms near silver and gold. To summarize the discussion, although our result at 1 nm is mostly qualitative, it clearly points to a potentially interesting platform for studying nonlocal, nondipolar, and nonperturbative light–matter interactions in graphene plasmonics.

PHYSICS OF THE LAMB SHIFT IN GRAPHENE

We conclude our study of using the graphene Lamb shift to tune atomic spectra by discussing the different contributions to the Lamb shift and illustrating the origin of the Fermi energy resonances.

Plasmon, Intraband, and Particle-Hole Contributions to the Lamb Shift. In order to get an approximate sense of where different contributions to the graphene Lamb shift come from, we examine in Figure 4 the differential Lamb shift, $d\delta E/d\omega$, which is defined to be the integrand of eq 1. Noting that this integrand is proportional to the imaginary part of the Green function for the air–graphene–substrate system, the differential Lamb shift can also be written in terms of the more familiar Purcell factor via

$$\frac{d\delta E_a}{d\omega} = \frac{2\alpha\hbar}{3\pi c^2}\omega^3 D_{ij} F_p(\mathbf{r}_0, \omega)\left(\frac{(r_i r_j)^{aa}}{\omega} + \sum_b \frac{r_i^{ab} r_j^{ba}}{\omega_{ab} - \omega}\right) \tag{3}$$

where $D = \mathrm{diag}(1/2, 1/2, 1)$ and $F_p(\mathbf{r}_0, \omega)$ is the Purcell factor for a dipole polarized perpendicular to the graphene sheet at frequency ω and position $\mathbf{r}_0$. In Figure 4, we plot both the frequency-dependent Purcell factor and the differential Lamb shift as a function of frequency for two cases. In the first case a Hydrogen atom 6s state for an atom-surface separation of 5 nm (a) and 1 nm (b). In the second case, a two-level system with dipole moment (1 nm × $e \approx$ 7.4 D) and energy gap 0.3 eV at distance 5 nm (c) and 1 nm (d) away. In both the hydrogenic atom and the two-level system, while most of the Purcell factor comes from frequencies having plasmonic response ($\hbar\omega < 2E_F$, denoted by the blue-shaded area), the Lamb shift can have sizable contributions: >20% for 5 nm and up to 60% for 1 nm, from fluctuations having energies above $2E_F$. These fluctuations are associated with particle-hole excitations. From comparing the figures on the left-hand side and right-hand side, it is clear that the relative contribution of the plasmons and the particle-hole excitations also depend strongly on the atom-graphene separation. This is because when graphene plasmons dominate the Lamb shift, the frequency of the plasmon that has the largest contribution to the Lamb shift is roughly $\omega^* \sim \frac{1}{\sqrt{z_0}}$. However, as z_0 gets smaller, ω^* gets closer to $\frac{2E_F}{\hbar}$ and leads to a larger contribution from particle-hole excitations. We thus conclude from Figure 4 that at such low distances (1 nm for example, but generally below $1/k_F$), accurate modeling of the graphene plasmons takes an increasing role. In particular, the Drude model would miss the particle-hole contributions, while the local random phase approximation is expected to catch them. At even shorter distances, a nonlocal RPA would be the most appropriate model.

To conclude this discussion on the different contributions to the graphene Lamb shift, we briefly note that the intraband contributions arising from the Drude relaxation time of 100 fs were not too important. In the particular case of Figure 4, most of the difference between the full local conductivity model and a lossless Drude model came from interband terms. Because these intraband and interband losses were taken into account in Figure 3, it means that the tunability of the graphene Lamb shift is not compromised by losses. We note that a relaxation time of 100 fs is not particularly optimiztic, given that higher relaxation times have been experimentally observed recently.[22]

DOI: 10.1021/acsphotonics.7b00731
ACS Photonics 2017, 4, 3098–3105

Fermi Energy Resonances. Finally, we show how Figure 4 can be used to determine the position of the resonances in the Lamb shift that appear as the Fermi energy is varied. We notice from eq 3 that the differential Lamb shift consists of two parts: $F_p(\omega)$ and $\frac{1}{E_a - E_b - \hbar\omega}$, where $E_a - E_b = \hbar\omega_{ab}$. The Purcell factor part can achieve a maximum at some frequency ω_m, which can depend on the atom-graphene separation and graphene Fermi energy. When $E_a - E_b - \hbar\omega_m \approx 0$ for some intermediate state b, we expect that a resonance appears and the Lamb shifts becomes large, which then leads to the peak in Figure 3 (to be more precise, we want ω_m to be slightly smaller than $\frac{E_a - E_b}{\hbar}$). This peak can be considered to be due to the resonance between the energy of a graphene plasmon and the discrete transition energy from state a to state b. We emphasize that this mechanism for maximizing the Lamb shift (achieving a resonance between an atomic transition and a Purcell-factor-maximizing frequency) is extremely general and can be used as a design principle for optimizing Lamb shifts in any nanophotonic system, although here, we apply it to the specific case of graphene.

For graphene described by the local RPA, it is not possible to find an exact analytic form for the resonance position. Here, we provide an approximate result by finding ω_m as a function of E_F approximately, and setting $E_a - E_b - \hbar\omega_m = 0$. First of all, for each transition from a to b, there is always a sharp dip in the Lamb shift as a function of Fermi energy, which is at the location $E_F^{dip} = \frac{E_a - E_b}{2}$. Below this Fermi energy value, a large number of particle-hole excitations can be generated, which leads to a sharp change in the Lamb shift. We make note of this because to describe the position of the resonance $E_F^{(ab)}$, it is better to describe its position using its distance to this dip, which is $E_F^{(ab)} - \frac{E_a - E_b}{2}$. Assuming this to be small, a first order calculation gives $E_F^{(ab)} - \frac{E_a - E_b}{2} \approx (E_a - E_b)e^{-2+4\pi\epsilon_0\bar{\epsilon}_r z_0/q_c^2(E_a - E_b)}$. Again, this approximation correctly describes the distance dependence of the peak. By matching to the calculated numerical value, a more accurate expression for the peak position obtained from the calculated exact numerical values is $E_F^{(ab)} - \frac{E_a - E_b}{2} \approx (E_a - E_b)\mathrm{Be}^{A4\pi\epsilon_0\bar{\epsilon}_r z_0/q_c^2(E_a - E_b)}$. The correction numerical factors are $A \approx 0.4$ and $B \approx 0.1$. The above approximate form of the peak position can help us determine the resonance Fermi energy for other states or other atomic systems. Even though the numerical factors can be different we expect that the dependence on z_0 and $E_a - E_b$ should be the same.

SUMMARY

In summary, we have examined the potential for using tunable 2D nanophotonics platforms such as graphene to redesign the level structure of an emitter using the Lamb shift associated with both plasmonic and particle-hole excitations in graphene. We note that while the magnitude of the Lamb shift is similar to that which can be achieved through the physically equivalent van der Waals effect in metals like silver or gold, the degree of tunability of the Lamb shift for an emitter at a fixed position can be quite large. This potentially allows one to reorient the levels of an emitter by a few meV either in the positive or negative direction, or even not at all with a suitable choice of Fermi energy. Additionally, using this degree of freedom, by placing an emitter at increasingly closer distances to the surface (a couple of nm), one could potentially tune the Lamb shift between being zero, or being nearly as large as the energy gap itself, bringing one into a nonlocal, nondipolar, and non-perturbative regime of atom-field interactions—a regime of light-matter interactions which is notoriously difficult to study theoretically. Thus, the ability to tune the energy level structure of emitters through the Fermi energy could perhaps not only be of practical use for reorienting unfavorable energy level diagrams, but also providing a platform to controllably study strong light-matter interactions between atoms and 2D materials. We conclude with one last admittedly speculative comment, related to the fact that the chemical properties of an electronic system are intricately tied to the energy levels and wave functions. Therefore, it could perhaps be possible to controllably alter the chemical properties of an atom through the Lamb shift in graphene or other tunable optical environments.

ASSOCIATED CONTENT

Supporting Information

The Supporting Information is available free of charge on the ACS Publications website at DOI: 10.1021/acsphotonics.7b00731.

Equivalence of the Hamiltonians in **A** and **E** representations; Expression of the Lamb shift; derivation of the distance scaling law; Derivation of the resonant Fermi energy position in lossless and lossy cases; Cutoff dependence of the Lamb shift; Comparison of the lossless Drude model and the local RPA model; Distance dependence of the quadrupole shift (PDF).

AUTHOR INFORMATION

Corresponding Author

*E-mail: nrivera@mit.edu.

ORCID

Nicholas Rivera: 0000-0002-8298-1468

Notes

The authors declare no competing financial interest.

ACKNOWLEDGMENTS

Research supported as part of the Army Research Office through the Institute for Soldier Nanotechnologies under contract no. W911NF-13-D-0001 (photon management for developing nuclear-TPV and fuel-TPV mm-scale-systems). Also supported as part of the S3TEC, an Energy Frontier Research Center funded by the US Department of Energy under grant no. DE-SC0001299 (for fundamental photon transport related to solar TPVs and solar-TEs). The work by I.K. was supported in part by the MRSEC Program of the National Science Foundation under award number DMR - 1419807. The research of I.K. was also partially supported by the Seventh Framework Programme of the European Research Council (FP7-Marie Curie IOF) under Grant agreement No. 328853-MC-BSiCS. N.R. was supported by a Department of Energy fellowship no. DE-FG02-97ER25308.

REFERENCES

(1) Dirac, P. A. The quantum theory of the emission and absorption of radiation. *Proc. R. Soc. London, Ser. A* **1927**, *114*, 243–265.

(2) Bethe, H. A. The electromagnetic shift of energy levels. *Phys. Rev.* **1947**, *72*, 339.

DOI: 10.1021/acsphotonics.7b00731
ACS Photonics 2017, 4, 3098–3105

(3) Lamb, W. E.; Retherford, R. C. Fine structure of the Hydrogen atom by a microwave method. *Phys. Rev.* **1947**, *72*, 241.
(4) Ribeiro, S.; Buhmann, S. Y.; Stielow, T.; Scheel, S. Casimir-Polder interaction from exact diagonalization and surface-induced state mixing. *Europhys. Lett.* **2015**, *110*, 51003.
(5) Anderson, A.; Haroche, S.; Hinds, E. A.; Jhe, W.; Meschede, D. Measuring the van der Waals forces between a Rydberg atom and a metallic surface. *Phys. Rev. A: At., Mol., Opt. Phys.* **1988**, *37*, 3594.
(6) Sandoghdar, V.; Sukenik, C. I.; Hinds, E. A.; Haroche, S. Direct measurement of the van der Waals interaction between an atom and its images in a micron-sized cavity. *Phys. Rev. Lett.* **1992**, *68*, 3432.
(7) Landragin, A.; Courtois, J. Y.; Labeyrie, G.; Vansteenkiste, N.; Westbrook, C. I.; Aspect, A. Measurement of the van der Waals force in an atomic mirror. *Phys. Rev. Lett.* **1996**, *77*, 1464.
(8) Barton, G. Frequency shifts near an interface: inadequacy of two-level atomic models. *J. Phys. B: At. Mol. Phys.* **1974**, *7*, 2134.
(9) Meschede, D.; Jhe, W.; Hinds, E. A. Radiative properties of atoms near a conducting plane: An old problem in a new light. *Phys. Rev. A: At., Mol., Opt. Phys.* **1990**, *41*, 1587.
(10) Barton, G. Quantum electrodynamics of atoms between parallel mirrors. *Phys. Scr.* **1988**, *21*, 11.
(11) Alves, D. T.; Barone, F. A.; Farina, C.; Tort, A. C. Influence of two parallel plates on atomic levels. *Phys. Rev. A: At., Mol., Opt. Phys.* **2003**, *67*, 022103.
(12) Sun, Q.; Al-Amri, M.; Kamli, A.; Zubairy, M. S. Lamb shift due to surface plasmon polariton modes. *Phys. Rev. A: At., Mol., Opt. Phys.* **2008**, *77*, 062501.
(13) Yao, P.; Van Vlack, C.; Reza, A.; Patterson, M.; Dignam, M. M.; Hughes, S. Ultrahigh Purcell factors and Lamb shifts in slow-light metamaterial waveguides. *Phys. Rev. B: Condens. Matter Mater. Phys.* **2009**, *80*, 195106.
(14) Matloob, R. Quantum-electrodynamic level shifts in an absorbing medium. *Phys. Rev. A: At., Mol., Opt. Phys.* **2000**, *61*, 062103.
(15) Vats, N.; John, S.; Busch, K. Theory of fluorescence in photonic crystals. *Phys. Rev. A: At., Mol., Opt. Phys.* **2002**, *65*, 043808.
(16) Sakoda, K. *Optical Properties of Photonic Crystals*; Springer, 2001.
(17) Wang, X. H.; Kivshar, Y. S.; Gu, B. Y. Giant Lamb shift in photonic crystals. *Phys. Rev. Lett.* **2004**, *93*, 073901.
(18) Li, Z. Y.; Xia, Y. Optical photonic band gaps and the Lamb shift. *Phys. Rev. B: Condens. Matter Mater. Phys.* **2001**, *63*, 121305.
(19) Zhu, S. Y.; Yang, Y.; Chen, H.; Zheng, H.; Zubairy, M. S. Spontaneous radiation and lamb shift in three-dimensional photonic crystals. *Phys. Rev. Lett.* **2000**, *84*, 2136.
(20) Artoni, M.; La Rocca, G.; Bassani, F. Resonantly absorbing one-dimensional photonic crystals. *Phys. Rev. E* **2005**, *72*, 046604.
(21) Liu, Q.; Song, H.; Wang, W.; Bai, X.; Wang, Y.; Dong, B.; Xu, L.; Han, W. Observation of Lamb shift and modified spontaneous emission dynamics in the YBO_3: Eu^{3+} inverse opal. *Opt. Lett.* **2010**, *35*, 2898−2900.
(22) Woessner, A.; Lundeberg, M. B.; Gao, Y.; Principi, A.; Alonso-González, P.; Carrega, M.; Watanabe, K.; Taniguchi, T.; Vignale, G.; Polini, M.; Hone, J. Highly confined low-loss plasmons in graphene boron nitride heterostructures. *Nat. Mater.* **2014**, *14*, 421−425.
(23) Fei, Z.; Rodin, A. S.; Andreev, G. O.; Bao, W.; McLeod, A. S.; Wagner, M.; Zhang, L. M.; Zhao, Z.; Dominguez, G.; Thiemens, M.; Fogler, M. M. Gate-tuning of graphene plasmons revealed by infrared nano-imaging. *Nature* **2012**, *487*, 82−85.
(24) Fei, Z.; Andreev, G. O.; Bao, W.; Zhang, L. M.; McLeod, A. S.; Wang, C.; Stewart, M. K.; Zhao, Z.; Dominguez, G.; Thiemens, M.; Fogler, M. M. Infrared nanoscopy of Dirac plasmons at the graphene−SiO_2 interface. *Nano Lett.* **2011**, *11*, 4701−4705.
(25) Koppens, F. H.; Chang, D. E.; García de Abajo, F. J. Graphene plasmonics: a platform for strong light−matter interactions. *Nano Lett.* **2011**, *11*, 3370−3377.
(26) Vakil, A.; Engheta, N. Transformation optics using graphene. *Science* **2011**, *332*, 1291−1294.
(27) Tielrooij, K. J.; Orona, L.; Ferrier, A.; Badioli, M.; Navickaite, G.; Coop, S.; Nanot, S.; Kalinic, B.; Cesca, T.; Gaudreau, L.; Ma, Q. Electrical control of optical emitter relaxation pathways enabled by graphene. *Nat. Phys.* **2015**, *11*, 281−287.
(28) Kim, S.; Jang, M. S.; Brar, V. W.; Mauser, K. W.; Atwater, H. A. Electronically Tunable Perfect Absorption in Graphene. *arXiv:1703.03579* **2017**, na.
(29) Muschik, C. A.; Moulieras, S.; Bachtold, A.; Koppens, F. H.; Lewenstein, M.; Chang, D. E. Harnessing vacuum forces for quantum sensing of graphene motion. *Phys. Rev. Lett.* **2014**, *112*, 223601.
(30) Kaminer, I.; Katan, Y. T.; Buljan, H.; Shen, Y.; Ilic, O.; López, J. J.; Wong, L. J.; Joannopoulos, J. D.; Soljačić, M. Efficient plasmonic emission by the quantum Cerenkov effect from hot carriers in graphene. *Nat. Commun.* **2016**, *7*, 7.
(31) Rivera, N.; Kaminer, I.; Zhen, B.; Joannopoulos, J. D.; Soljačić, M. Shrinking light to allow forbidden transitions on the atomic scale. *Science* **2016**, *353*, 263−269.
(32) Cohen-Tannoudji, C.; Dupont-Roc, J.; Grynberg, G.; Thickstun, P. *Atom-Photon Interactions: Basic Processes and Applications*; Wiley, 1992.
(33) Novotny, L.; Hecht, B. *Principles of Nano-Optics*; Cambridge University Press, 2012.
(34) Jablan, M.; Soljačić, M.; Buljan, H. Plasmons in graphene: fundamental properties and potential applications. *Proc. IEEE* **2013**, *101*, 1689−1704.

DOI: 10.1021/acsphotonics.7b00731
ACS Photonics 2017, 4, 3098−3105